



HAL
open science

Water-rock interactions and self-remediation: Lessons from a hydraulic fracturing operation in the Vaca Muerta formation, Argentina

F. Osselin, E.C. Gaucher, P. Baldony-Andrey, Wolfram Kloppmann, B. Mayer

► To cite this version:

F. Osselin, E.C. Gaucher, P. Baldony-Andrey, Wolfram Kloppmann, B. Mayer. Water-rock interactions and self-remediation: Lessons from a hydraulic fracturing operation in the Vaca Muerta formation, Argentina. *Geoenery Science and Engineering*, 2023, 224, pp.211496. 10.1016/j.geoen.2023.211496 . insu-03978645

HAL Id: insu-03978645

<https://insu.hal.science/insu-03978645v1>

Submitted on 8 Feb 2023

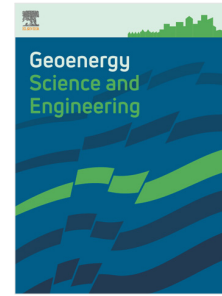
HAL is a multi-disciplinary open access archive for the deposit and dissemination of scientific research documents, whether they are published or not. The documents may come from teaching and research institutions in France or abroad, or from public or private research centers.

L'archive ouverte pluridisciplinaire **HAL**, est destinée au dépôt et à la diffusion de documents scientifiques de niveau recherche, publiés ou non, émanant des établissements d'enseignement et de recherche français ou étrangers, des laboratoires publics ou privés.

Journal Pre-proof

Water-rock interactions and self-remediation: Lessons from a hydraulic fracturing operation in the Vaca Muerta formation, Argentina

F. Osselin, E.C. Gaucher, P. Baldony-Andrey, W. Kloppmann,
B. Mayer



PII: S2949-8910(23)00083-0
DOI: <https://doi.org/10.1016/j.geoen.2023.211496>
Reference: GEOEN 211496

To appear in: *Geoenergy Science and Engineering*

Received date: 3 June 2022
Revised date: 21 December 2022
Accepted date: 24 January 2023

Please cite this article as: F. Osselin, E.C. Gaucher, P. Baldony-Andrey et al., Water-rock interactions and self-remediation: Lessons from a hydraulic fracturing operation in the Vaca Muerta formation, Argentina. *Geoenergy Science and Engineering* (2023), doi: <https://doi.org/10.1016/j.geoen.2023.211496>.

This is a PDF file of an article that has undergone enhancements after acceptance, such as the addition of a cover page and metadata, and formatting for readability, but it is not yet the definitive version of record. This version will undergo additional copyediting, typesetting and review before it is published in its final form, but we are providing this version to give early visibility of the article. Please note that, during the production process, errors may be discovered which could affect the content, and all legal disclaimers that apply to the journal pertain.

© 2023 Elsevier B.V. All rights reserved.

Water-rock interactions and self-remediation: lessons from a hydraulic fracturing operation in the Vaca Muerta formation,

Argentina

F. Osselin^{1,*}, E.C. Gaucher^{2,+}, P. Baldony-Andrey², W. Kloppmann⁴, and B. Mayer³

¹Institut des Sciences de la Terre d'Orléans, Université d'Orléans, CNRS, BRGM
UMR7327, 1A Rue de la Ferrollerie, 45100 Orléans, France

²TotalEnergies, France

³Applied Geochemistry Group, Department of Geoscience, University of Calgary, 2500
University Dr. NW, Calgary, Alberta, T2N 1N4, Canada

⁴French Geological Survey (BRGM), Orléans, France

*Corresponding author

⁺Present address: RWI Group, Institute of Geological Science, University of Bern,
Switzerland

January 25, 2023

1 Abstract

2 In order to analyze the effect of a new gelling agent for hydraulic fracturing, fluid samples from different
3 stages of the operation (hydraulic fracturing fluid, coil tubing, flowback and produced waters) were col-
4 lected from a well in the the Vaca Muerta formation in Argentina. Collected samples were analyzed for
5 major and trace elements, first within a few days after sampling, then reanalyzed 6 months later and again
6 2 years after sampling. Results show that the salinity of samples increased quickly with time, from 2000
7 mg/L up to 43,000 mg/l a month later, due to the mixing of hydraulic fracturing fluids with formation

8 water. No evidence of water-rock reactions was observed. Results from the later analyses showed that the
9 composition of the samples evolved with time with a sensible decrease of concentration for most trace ele-
10 ments over the course of these two years (e.g. Ba from 137 mg/L to 55 mg/L, Mn from 8mg/L to 5mg/L)
11 and heavy metals (e.g. As 100 μ g/L to 1 μ f/L, Co 160 μ g/L to 1.4 μ g/L, Cr from 160 μ g/L to 26 μ g/L). Inter-
12 pretation of the results shows that delayed, post-sampling, precipitation of barite in the preserved samples
13 is the reason for such a decrease. This opens a very interesting option for mitigation and remediation of
14 wastewaters from hydraulic fracturing as natural or even triggered precipitation of barite could involve
15 most of the dissolved heavy metals and decrease strongly their concentrations.

16 2 Introduction

17 The exploitation of hydrocarbons trapped in tight formations is continuing its worldwide expansion with
18 countries like USA or Canada producing a large percentage of their hydrocarbon resources through shale
19 gas plays like the Marcellus, Eagle Ford, Permian Basin formations in the United-States (, EIA), the Mont-
20 ney, Duvernay and Horn River formations in Canada (Board, 2017; of Canada, 2018; of Canadian Academies,
21 2014). Numerous other countries are joining the movement, with recent hydraulic fracturing operations
22 in Argentina where the giant reservoir of Vaca Muerta was discovered in 2010 (Administration, 2013) is
23 exploited.

24 Hydraulic fracturing and the exploitation of shale gas can appear as a controversial technology and its
25 global expansion is met with criticism from ecological organizations (Brittingham et al., 2014). Indeed,
26 concerns remain about the potential contamination of freshwater resources by fugitive methane emana-
27 tions (Osborn et al., 2011; Humez et al., 2019) or by hydraulic fracturing fluids migration (Darrah et al.,
28 2014; Warner et al., 2012; Bondu et al., 2021). Other environmental risks are linked to the very high water
29 consumption (Gallegos and Varela, 2015; Gregory et al., 2011a; Vengosh et al., 2014; Kondash et al., 2018),
30 as well as the treatment and recycling of thousands of cubic meters of potentially toxic wastewaters pro-
31 duced per well (Thiel et al., 2015; Gregory et al., 2011b). Indeed, after hydraulic fracturing of the reservoir,
32 when the well is opened to production, a large quantity of water (called flowback water) is produced (Kon-
33 dash et al., 2017). These fluids are a mixture of hydraulic fracturing fluids with formation brine as well
34 as products of water-rock interactions, the latter being frequently enhanced by the additives used for the
35 optimization of the hydraulic fracturing operation itself (Osselin et al., 2018, 2019; Birkle, 2016; Birkle and
36 Makechnie, 2022; Li et al., 2017; Lu et al., 2017; Phan et al., 2020). These flowback fluids are characterized

37 by a very high TDS (total dissolved solids), usually several times the salinity of seawater and contain usu-
38 ally non-negligible quantities of trace elements and heavy metals (e.g. As, Ni, Co, Cr) with a potentially
39 high toxicity (Haluszczak et al., 2013; Blauch et al., 2009; Abualfaraj et al., 2014; Phan et al., 2015; Johnson
40 and Graney, 2015; Ni et al., 2018; Bern et al., 2021). The disposal and remediation of these high salinity
41 fluids is complicated and operators usually choose to reinject these fluids underground in nearby porous
42 formations, usually into stratigraphically deep reservoirs, well below aquifers utilized for water supplies.
43 However, considering the very high consumption of freshwater by hydraulic fracturing operations (several
44 thousand cubic meters per stage), and especially in areas where the freshwater resource is already under
45 strain, there is a strong incentive to recycle and reuse these flowback fluids for the next hydraulic fracturing
46 operation (Liu et al., 2020). One way to simplify the processing of flowback fluids for reuse in hydraulic
47 fracturing operations is to control the downhole water-rock interactions and the release of heavy metal
48 and traces by the formation (Osselin et al., 2019; Lerat et al., 2018). An extensive understanding of the
49 downhole geochemical behavior during hydraulic fracturing and subsequent flowback is then required in
50 order to optimize and tailor the geochemistry of flowback fluids. In particular, it was shown that the use
51 of oxidative breakers was not optimal because of its very aggressive behavior towards minerals like pyrite
52 and organic matter releasing heavy metals in the flowback fluids (Renock et al., 2016; Yang et al., 2021).

53 This study presents the analysis of flowback samples from a well operated in Argentina. This well
54 presents the particularity of having been treated with a novel fracturing fluid mixture, not involving the
55 classic couple guar gum and oxidant breaker. Instead, the gelling agent (i.e. the additive modifying vis-
56 cosity for a better proppant transport into the fractures) was composed of fragile polymers. Upon opening
57 the well to production, when a lower viscosity is desirable for smooth flowback (i.e., once the proppant
58 has been transported deep into the hydraulic fractures), the decrease in viscosity is not achieved by an ag-
59 gressive oxidative attack on the polymer but by a simple mechanical shearing and breaking of the polymer
60 due to the rough and intersected nature of the hydraulic fractures network. If the polymer is forced into a
61 steep angle because of the geometry of the hydraulic fractures, it will break into smaller pieces. Thus the
62 downhole geochemistry is strongly different from other classic hydraulically fractured wells such as from
63 the Marcellus or the Montney shales, because of the absence of oxidative action on the sulfide minerals and
64 on organic matter.

65 Several water samples were collected during the different stages of the procedure, the hydraulic fractur-
66 ing itself, the coil tubing operation which opens the different stages to the main wellbore, and finally the
67 flowback once the well is opened to production. All samples were analyzed for major elements and traces

68 as well as several stable isotopes in order to elucidate the downhole behavior and see if the absence of ox-
69 idative breaker was impacting beneficially the overall composition of returned waters in view of recycling
70 and reuse of such waters for further hydraulic fracturing operations or simply for disposal.

71 3 Material and Methods

72 **Study site and well completion** The considered well is located in the province of Neuquen, North-West
73 Patagonia, Argentina (Figure 1). The target formation is the Vaca Muerta formation, a carbonate marl with
74 black shale and lime mudstone. The targeted interval (between 2600 mbs (meters below surface) and 2800
75 mbs) presents an average composition of 15% albite feldspar ($\text{NaAlSi}_3\text{O}_8$), 30% quartz (SiO_2), 25% calcite
76 (CaCO_3), 22% illite (clay mineral), with a bit (3%) of pyrite (FeS_2) and traces of dolomite and apatite.

77 In this zone, several pads were constructed, with each pad being the starting point of three horizon-
78 tal wells in a two pronged fork shape. The horizontal portion of the studied well was divided into 15
79 stages. After the drilling of the well and the perforations, but before any hydraulic fracturing, the well was
80 spearheaded with HCl to cleanse debris and prepare the formation for the hydraulic fracturing operation.
81 Hydraulic fracturing was proceeded with a slickwater mixture with freshwater obtained from the overlying
82 sandstone aquifer. The water used came from two different wells labeled WW3 and WW4.

83 The 15 stages were proceeded from toe (the far end of the horizontal wellbore) to heel, and stages were
84 separated from each other by small aluminum plugs. After all stages were fractured, the well was subjected
85 to a coil-tubing operation to open the stages to production. This operation consists of inserting a flexible
86 drill into the horizontal wellbore and drilling the plugs which opens the stages. During this operation,
87 no water is produced and the whole system supposedly works as a closed loop. However, due to some
88 overheating of the water and the equipment, it was necessary to add four trucks of freshwater during the
89 operation with each truck containing 25m^3 of water. Before the addition, the same amount was bled from
90 the closed loop and replaced with the freshwater from the trucks. One truck was added between the 7th
91 and the 8th stage, another between the 13th and 14th stage and 2 trucks between 14th and the last plug for
92 a total of 100m^3 of freshwater (Figure 2).

93 Finally, the well was left to rest one week between the end of the coil-tubing operation and the beginning
94 of flowback (i.e. opening of the well to production).

95 **Analytical Methods** Samples were obtained on site during the coil-tubing procedure and the flowback
96 (Oct-Nov 2015). Samples from the water wells used for the hydraulic fracturing fluids (WW3 and WW4)



Figure 1: Location of the Neuquen region

97 were also obtained as well as one produced water sample from another hydraulically fractured well on
98 another pad, which was put to production four months before the operation on the considered well. This
99 sample, named PW, was considered to be representative of the formation brine. In total, three samples
100 were taken during coil-tubing (CT1, CT2 and CT3), one after the first plug was drilled, one between plugs
101 7 and 8, and one after the last plug was drilled. Unfortunately, the first CT sample was not kept. A total of
102 6 flowback (FB1 to FB6) samples were obtained during the first 2 days of flowback at regular intervals.

103 After filtration (0.1 μm), the pH of the samples was measured before being preserved on site (acidifica-
104 tion pH < 2 for cation analysis) and shipped a few days later to INDUSER (Induser Group SRL, Laboratory
105 of Chemical and Microbiological Analysis, Buenos Aires, Argentina) for analysis. Samples were analyzed
106 for all major and trace elements by the laboratory as well as numerous organic species. Cations were
107 quantified by ICP-OES (inductively coupled plasma optical emission spectrophotometer) and anion con-
108 centrations were measured by ion chromatography. Bicarbonate alkalinity was measured by titration. Total
109 dissolved solids (TDS) content was calculated by adding all measured concentrations of dissolved species
110 and the consistency of the results (QA/QC) was verified by checking that the ionic balance was below 5%
111 for all samples.

112 Stable isotope analysis were made at BRGM (French Geological Survey, Orléans, France). Water isotopes
113 ratios ($\delta^2\text{H}$ and $\delta^{18}\text{O}$) were determined by CF-IRMS (continuous flow isotope ratio mass spectrometry) and
114 results are reported in the δ notation $\delta = (R_{spl}/R_{std} - 1) \times 1000$, with R_{spl} the isotope ratio in the sample and
115 R_{std} the isotope ratio of a standard reference. For water isotopes, the standard reference is V-SMOW.

116 The exploitation of the results from INDUSER showed that the detection limits from this laboratory
117 were too high for the samples and very little could be read from these analyses (see Supplementary In-
118 formation Tables 1-4). Additional analyses were then requested for the trace elements with some done
119 at TOTALnergies (Laboratory of Inorganic Chemistry, CSTJF, Pau, France) and some at BRGM (French
120 Geological Survey). The TOTALnergies analyses were proceeded in July 2016 (i.e. 8 to 9 months after
121 sampling due to delays on the exportation of the samples). Concentrations of trace elements were measured
122 at BRGM on Thermo Scientific XSERIES 2 ICP-MS with a precision generally better than 5%. Analyses were
123 performed on April 2018 i.e. more than 2 years after sampling. Finally, radium quantification was made
124 by ALGADE by gamma-spectrometry, using Pb214 and Bi214 for Ra226 and Ac228 for Ra228 according to
125 the norm NF EN ISO 550 1070. Analyses were proceeded on 3 samples (PW, FB1 and FB6) in August 2016
126 i.e. 9 months after sampling.

127 **QA/QC** The quality of trace element analyses is highly dependent on the quality of sample preparation on
128 site. Samples were routinely filtered with a 0.1 μm pore size syringe filter, following the recommendation
129 of Claret et al. (2011) to avoid conventional filters with larger pore sizes 0.2 μm or 0.45 μm . Filtration was
130 performed immediately after fluid sampling on the borehole fluid circulation loop.

131 A QC check of the analyses was performed by checking with PHREEQC (Appelo and Postma, 2005;
132 Parkhurst and Appelo, 2013), the charge balances and the equilibrium of the fluids with calcite. As this
133 equilibrium is usually quickly reached in sedimentary systems and as calcite belongs to the mineralogy of
134 the considered formation, it demonstrates that pH, alkalinity and calcium concentration are correctly an-
135 alyzed and by extension major elements, based on the charge balance. For metals, redundancy of analyses
136 in different laboratories was planned as a means of quality control, but the results of this cross-check are
137 part of the discussion of the article.

138 4 Results

139 The behavior of the well can be divided into 2 phases: (i) the hydraulic fracturing and coil-tubing until
140 October 8th 2015 and (ii) flowback and production from Oct. 8th 2015 as represented on Figure 2. During
141 the first phase, the TDS increases by an order of magnitude, going from ≈ 1500 mg/L in the hydraulic
142 fracturing fluid (average between WW3 and WW4), to 13,978 mg/L for sample CT1 in the midst of coil-
143 tubing operations, and nearly doubling to 23,824 mg/L for CT2 at the end of coil-tubing. After the well is
144 opened to flowback, the first sample presents a TDS value almost identical to the end of CT (22,999 mg/L).
145 TDS increases quickly up to 41,996 mg/L after a few hours of flowback maintain stable for the remaining
146 flowback period (i.e. 48 hours).

147 Evolution of other major elements is represented on Figure 3 as a function of Cl, as chloride is usually
148 considered conservative during the whole duration of the process (Li et al., 2017; Engelder et al., 2014). The
149 goal of such a plot is to allow the identification of conservative and non-conservative species. Conservative
150 species will correlate linearly to Cl concentrations, while the absence of correlation indicates the presence
151 of mineral precipitation/dissolution and cation exchange.

152 All major elements are evolving similarly to the TDS content with an increase between hydraulic frac-
153 turing fluids and CT1 (e.g. Na from 650 mg/L to 5030 mg/L), a minor increase during CT (Na from 5030
154 mg/L to 7910 mg/L), followed by a small drop between CT and FB1 (from 7910 to 7820 mg/L). A fast
155 increase upon flowback (from 7820 to 13,550 mg/L) is followed by a period of almost no variation until the

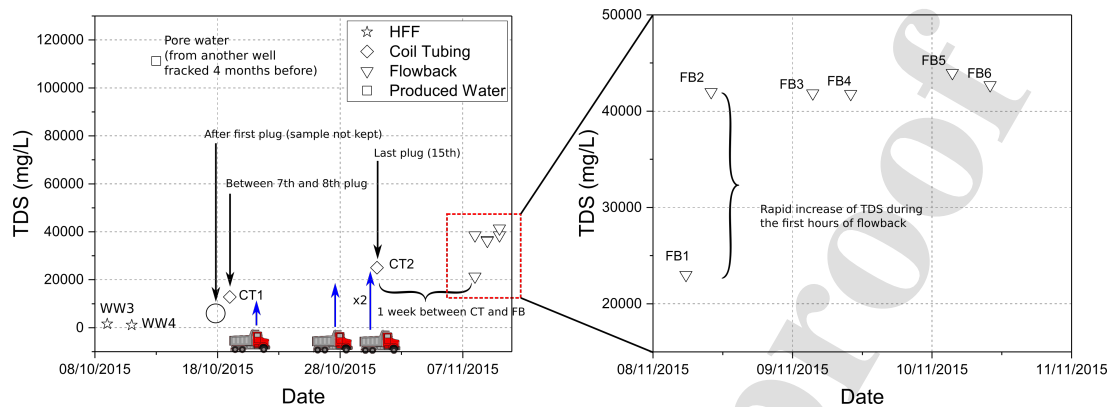


Figure 2: Evolution of TDS as a function of time during coil-tubing and flowback (INDUSER). The right figure shows a zoom of the flowback period

156 end of the sampling period. Interestingly, Na, Ca and Mg concentrations plot linearly with Cl for HFF,
 157 coil tubing and flowback samples, except sample PW which plots either higher for Ca, Mg, and lower for
 158 Na and K. Finally, the drop between CT2 and FB1 is proportionally more pronounced for K (from 87 mg/L
 159 down to 56.2 mg/L) than for the other major species respectively to Cl.

160 Alkalinity also shows an increase from 450 mg/L for the hydraulic fracturing fluid to 895 mg/L for CT1
 161 and up to 1480 mg/L for FB3. The PW value for the alkalinity is actually smaller than for the hydraulic
 162 fracturing fluid with a value of 136 mg/L.

163 Barium presents an increase in concentration similar to the major elements but does not seem to plot
 164 linearly with Cl (Fig. 4). The first coil-tubing sample shows a value almost at zero, when CT2 plots at
 165 23.9 mg/L and the flowback concentrations are around 135 mg/L. On the opposite, sulfate concentration is
 166 high for hydraulic fracturing fluids (300 mg/L) and drops quickly during coil-tubing (CT1 at 200 mg/L and
 167 CT2 at 106 mg/L) before reaching around 35 mg/L during flowback (Fig. 4). There is no value for sulfate
 168 concentration for FB1. Radium is measured at 1.58 Bq/L in the initial flowback sample and increased to
 169 13.65 Bq/L in the last flowback sample. The produced water sample presents a Ra activity of 137.3 Bq/L.

170 Water isotopes present a behavior similar to the major dissolved species, with a steady evolution from
 171 -88.8 and -95.3‰ for $\delta^2\text{H}$ values of respectively WW3 and WW4 to -66.5‰ at the end of coil-tubing, then
 172 -65.0‰ for FB1 and a plateau ratio around -53.5‰ for flowback samples after the first (Fig. 5). Oxygen
 173 isotope values increase from -11.0 and -12.3‰ in WW3 and WW4 samples up to -5.9‰ for CT2 and -6.0‰
 174 at the beginning of flowback. The flowback plateau is around -4‰. Finally the produced water sample PW
 175 is measured at $\delta^2\text{H} = -33.0‰$ and $\delta^{18}\text{O} = -1.5‰$. A cross-plot $\delta^{18}\text{O}$ versus $\delta^2\text{H}$ shows that WW3 and WW4

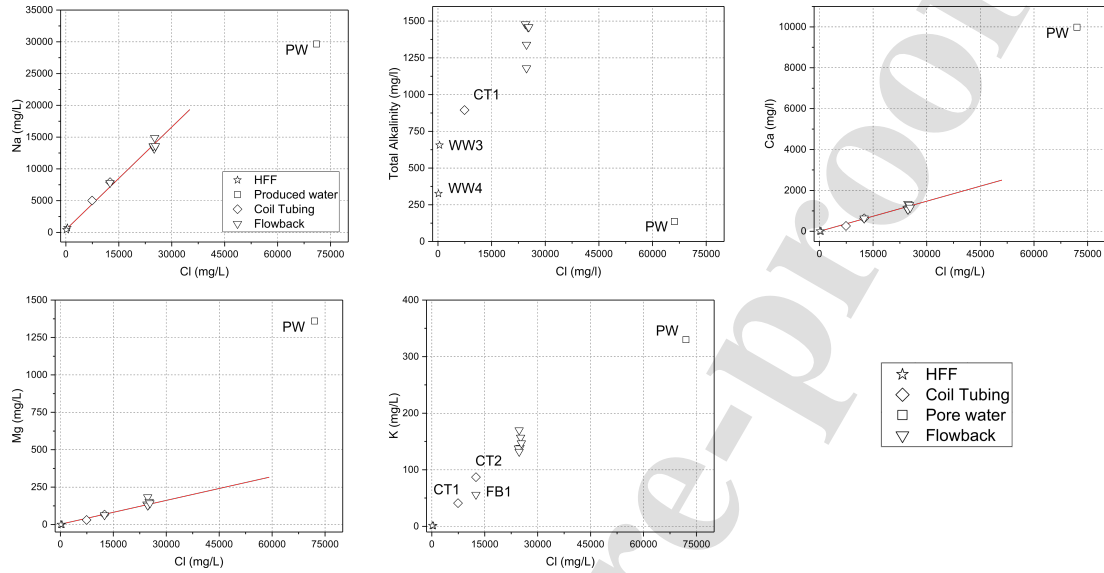


Figure 3: Plots of major species against Cl during coil-tubing and flowback (INDUSER)

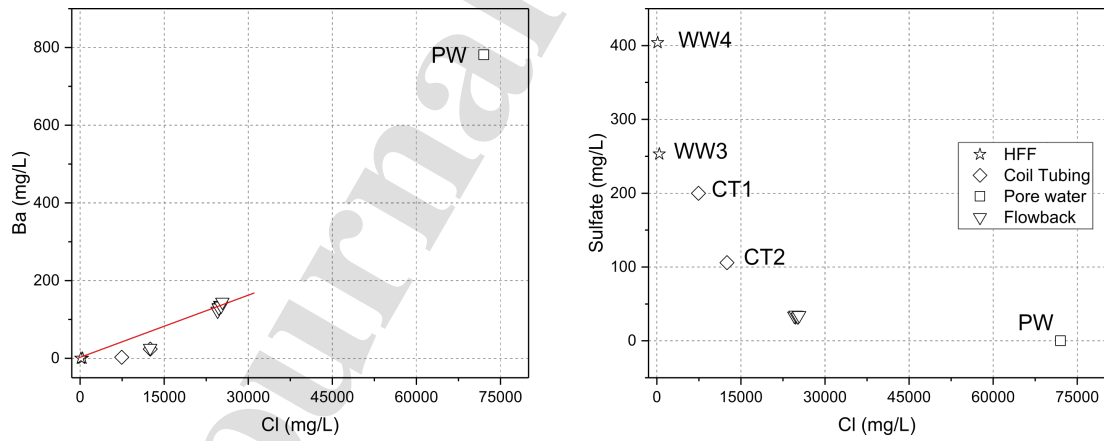


Figure 4: Plot of Ba and sulfate against Cl during coil-tubing and flowback (INDUSER)

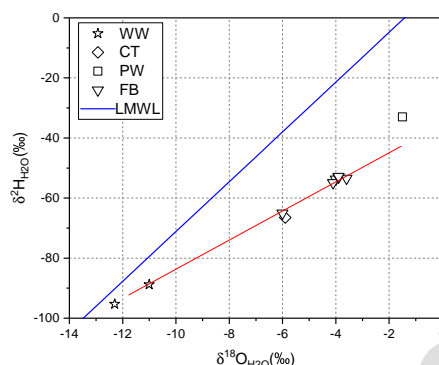


Figure 5: Cross plot of $\delta^2\text{H}$ vs $\delta^{18}\text{O}$ and the LMWL (BRGM)

176 plot close to the Local Meteoric Water Line (LMWL) (Hoke et al., 2013) while subsequent samples depart
177 from this line.

178 Few samples with heavy metals concentrations beyond the INDUSER detection limit (Nov. 2015)
179 present values between 100 and 200 $\mu\text{g/L}$. The highest values measured for heavy metals are 210 $\mu\text{g/L}$
180 for As in PW, 190 $\mu\text{g/L}$ for Co in FB1, 240 $\mu\text{g/L}$ for Cu in FB1, 200 $\mu\text{g/L}$ for Cr in CT2. Mn presents val-
181 ues between 5 and 15 mg/L, B up to 85 mg/L for FB4 and Fe up to 200 mg/L for FB5. However, values
182 measured from BRGM (April 2018) differ strongly. For example 0.67 $\mu\text{g/L}$ of As in PW, 1.4 $\mu\text{g/L}$ of Co in
183 FB2, 1.7 $\mu\text{g/L}$ of Cu in FB2 and 22.9 $\mu\text{g/L}$ of Cr in CT2. For boron, FB samples drop from around 80 mg/L
184 to 50 mg/L, while CT2 increases from 31.1 mg/L to 65.2 mg/L between INDUSER and BRGM results. Mn
185 decreases from 7.5-8 mg/L in flowback to 5.5 mg/L and from 5.1 mg/L to 1.668 mg/L in sample CT2 (Fig-
186 ure 6). Only three samples were quantified for Fe in BRGM, with sample CT2 presenting the largest drop
187 between 97.1 mg/L for INDUSER down to 12 mg/L for BRGM, while PW concentrations decrease from 173
188 mg/L to 155 mg/L. The concentrations of Fe in FB3 does not change with 122 and 125 mg/L in INDUSER
189 and BRGM analysis respectively.

190 Similarly Ba shows a decrease in concentration from INDUSER to TOTAL (July 2016) to BRGM for
191 each sample, with drops between 15% of the initial value (PW) and around 60% for FB values (Figure
192 6). Strontium presents a similar behavior, to the exception of PW with an increase from 1750 mg/L for
193 INDUSER results up to 3002 mg/L in TOTAL analysis towards 2863.2 mg/L.

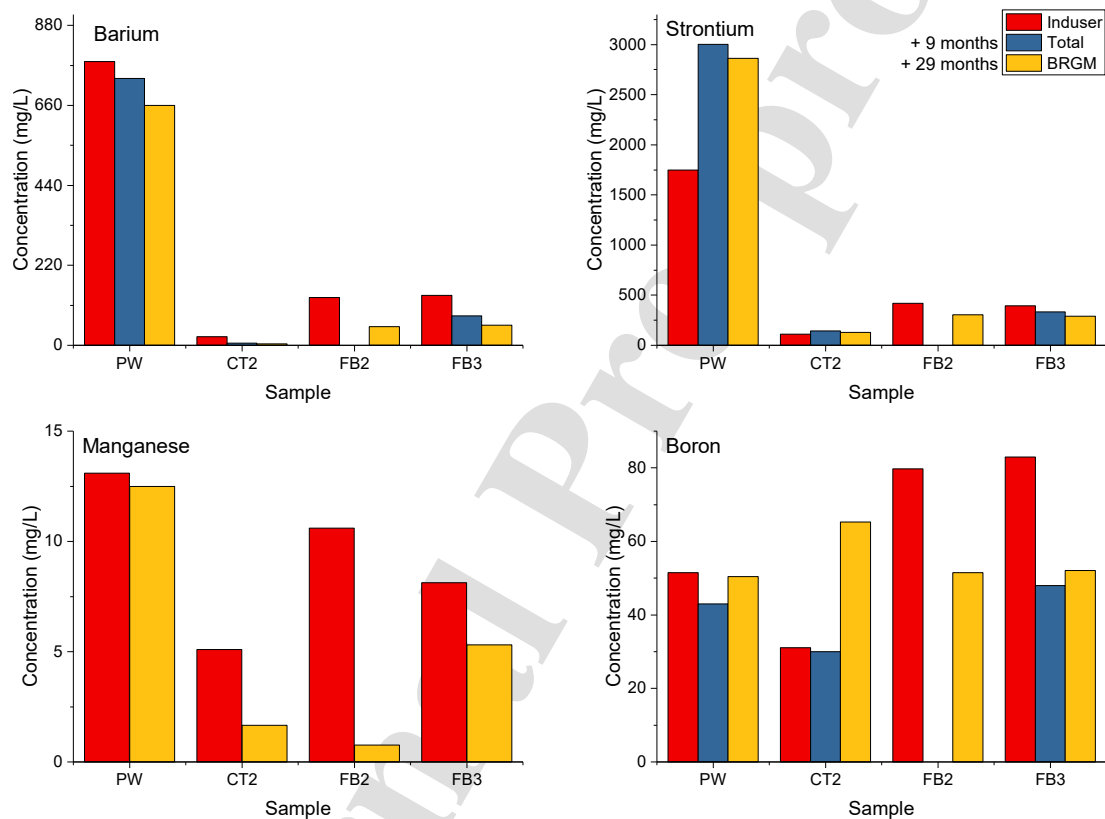


Figure 6: Evolution of Ba, Sr, Mn and B with time (i.e. according to the different laboratories). Error bars are significantly smaller than the variation (e.g. 1mg/L Induser and 0.5 μ g/L BRGM for Ba)

194 5 Discussion

195 **TDS and water-rock interactions** The evolution of salinity in flowback water has been extensively de-
196 scribed in numerous publications and is the result of mixing of the hydraulic fracturing fluids with forma-
197 tion brine as well as caused by chemical interactions between hydraulic fracturing fluid/formation water
198 and reservoir rock (Osselin et al., 2018; Rowan et al., 2015; Hakala et al., 2021; Huang et al., 2020). These
199 reactions usually involve salt dissolution if present in the mineralogy (halite, gypsum, anhydrite, calcite,
200 dolomite) and potential oxidation of sulfide minerals (pyrite FeS_2) and organic matter from fracturing wa-
201 ter containing strong oxidants (O_2 , oxidant breaker) (Osselin et al., 2019; Xu et al., 2018).

202 In the studied case, it is necessary to differentiate the behavior during coil-tubing from flowback. After
203 hydraulic fracturing, the injected fluid stays in the fractures during the whole coil-tubing operation as there
204 is no fluid production. The only exception is the addition of freshwater to cool down the fluid, which was
205 preceded by bleeding of the same volume of water from the well. As a result, since the bleeding decreased
206 the quantity of water in the fractures, a small proportion of formation water was allowed into the hydraulic
207 fractures and mixed with the hydraulic fracturing fluid. This explains the increase of TDS for samples CT1
208 and CT2 compared to WW3 and WW4. At the end of CT, the system was left to rest for a week with little
209 change in water composition. As no fluid was produced, no formation water was allowed in the system and
210 no change of TDS is detectable. This is another confirmation that the source of high TDS in flowback water
211 is not only the dissolution of autochthonous salts but mostly the mixing with high TDS formation brine.
212 The only remarkable feature between CT2 and FB1 is the small drop of K which is likely due to some cation
213 exchange with the clay minerals of the reservoir, e.g. replacement of Ca by K in the exchangeable sites of
214 the illite fraction (Essington, 2005).

215 Then, as the well is opened and flowback begins, a very fast increase of TDS is observed as the forma-
216 tion brine starts mixing with the hydraulic fracturing fluid. This increase is followed by a plateau where
217 flowback water salinity stays roughly the same. One of the reasons of this plateau is that almost all the
218 easily mobilized formation brine (i.e. mobile formation water close to the hydraulic fractures, probably in
219 natural fractures) already mixed with the fracturing fluids between FB1 and FB2. After that point, the mix-
220 ing slows down as the flow rate of formation water into the hydraulic fractures is smaller since the system
221 is tapping into tighter permeability rocks and less mobile sources of formation brine (Osselin et al., 2018).

222 Interestingly, pore water sample PW does not seem to correspond to the end-member for conservative
223 mixing. Indeed, water isotopes are considered conservative in this context (Rowan et al., 2015) and PW

224 does not fall (e.g. excess of +10‰ of $\delta^2\text{H}$) on a line joining the hydraulic fracturing fluids, coil tubing
225 fluids and flowback (Fig. 5). Since PW is a sample from another well fractured four months before, it
226 is possible that it does not correspond to the formation water of the considered well, either because four
227 months is potentially not long enough to reach the final composition of the formation water; because of
228 some interactions between wells shifting the global conservative mixing; or simply because the formation
229 water changes composition with the location of the well. Disregarding PW, it appears that Na, Ca, Mg and
230 K are likely to be conservative (to the exception of some cation exchange with the clay minerals), while
231 Ba and sulfate are probably not. Water isotopes further support this interpretation as they show a mostly
232 conservative mixing behavior during the whole coil-tubing and flowback duration (Fig. 5). The very similar
233 values in the water isotope ratios between CT2 and FB1 confirms the absence of mixing and water exchange
234 during the whole week between the end of coil-tubing and the beginning of flowback.

235 Saturation indexes of minerals have been modeled with PHREEQC v3 with the Pitzer database (Appelo,
236 2015) and results are represented in Figure 7. Calcite is at equilibrium for PW and or CT, but shows a slight
237 oversaturation for FB samples. This is perfectly consistent with the presence of calcite in the mineralogy of
238 the formation. A slight precipitation of calcite may then be expected but the simulation results confirm that
239 Na, Ca, Mg and K should be mostly conservative. The non-conservative behavior of Ba and sulfate can, on
240 the other hand, be explained by the oversaturation of barite during the whole duration of the operation. PW
241 – which can be considered as more or less representative of the formation brine despite not being the actual
242 end-member of the mixing in the considered well – is quite Ba-rich (781 mg/L), while the freshwater used
243 for the hydraulic fracturing operation is rather sulfate-rich (300 mg/L). Precipitation of barite is then likely,
244 especially with the addition of the four 25m³ trucks of sulfate-rich freshwater. The behavior of radium,
245 even in the absence of the first end-member can be linked to barium behavior: in the first flowback sample,
246 Ra and Ba are both very low due to barite precipitation incorporating Ra in the crystal structure (Scheiber
247 et al., 2014). Then the Ra concentration increases due to mixing with formation water.

248 Once the samples are preserved and acidified, calcite becomes strongly undersaturated and is not ex-
249 pected to precipitate. On the other hand, barite (BaSO_4) is not impacted by acidification and stays super-
250 saturated in all samples.

251 **Evolution of trace concentrations with time in preserved samples** As described in the result section, the
252 concentrations of heavy metals and trace elements vary widely between the three laboratories. Rejecting the
253 hypothesis that the analyses were erroneous, the reason for this discrepancy is that between the sampling

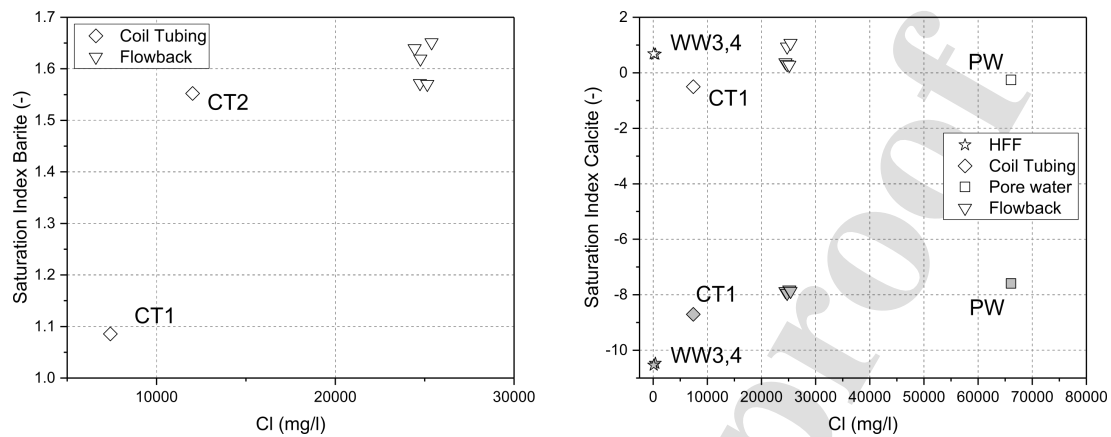


Figure 7: Evolution of barite and calcite saturation indices in the samples and the effect of acidification (Calculated from INDUSER data)

254 and the analyses, the samples were not really quenched by the acidification and evolved. Acidification is
 255 mainly used for preventing the precipitation of oxo-hydroxide iron complexes ($\text{Fe}(\text{OH})_3$) which are known
 256 to co-precipitate with other metallic cations (Appelo and Postma, 2005). However, as can be seen from the
 257 Ba evolution (Fig. 6 and from the SI from Figure 7, barite is very likely to have precipitated during the
 258 delayed analyses as its saturation index is not impacted by acidification. This precipitation plays a similar
 259 role as the iron oxo-hydroxides as barite co-precipitates with several traces such as Ra, As, Cu, Zn, Ag, Ni,
 260 Hg, Co, V, Pb, Mn and Cr and other rare-earth elements (Gupta, 1991; Crecelius et al., 2007). Most of the
 261 elements precipitate as a substitution to the Ba in the barite structure while some (Mn as permanganate
 262 MnO_4^- or Cr as chromate CrO_4^{2-}) substitute to sulfate (Tokunaga et al., 2016). This is consistent with
 263 the analytical results showing an overall decrease in all the mentioned cations as well as decrease of Ba
 264 with time. Strontium usually forms a solid solution with barite upon precipitation and presents indeed a
 265 decrease with time for all FB samples. The large increase between INDUSER and BRGM value for PW and
 266 CT2 is on the other hand not clear. As radium was only measured 9 months after sampling (similar time as
 267 TOTALEnergies analyses), it is likely that the actual values are higher than the ones measured.

268 Boron shows a similar increase with a large increase between INDUSER and BRGM results for CT2.
 269 One possible explanation is the slow decomposition of some colloidal complexes with time releasing Sr
 270 and B into solution (Appelo and Postma, 2005) during the 2 years between INDUSER and BRGM analyses.
 271 However the filtration on $0.10\mu\text{m}$ filters should not let some colloidal particles through. A damaged fil-
 272 ter, a mishandling of the samples or simply the difficulty associated with Boron analyses may explain the

273 discrepancy

274 The behavior of trace elements over these two years leads to two important conclusions:

- 275 • Acidification of samples is not enough to stabilize a sample with high sulfate and barium concentra-
276 tions. Analyses have to be made as soon as possible on flowback waters (or any high salinity brine
277 containing these two elements) in order to avoid any experimental error showing lower trace elements
278 concentration than in reality. Similarly, if the behavior of B and Sr is linked to the decomposition of
279 colloidal particles, then the filtration has also to be carefully controlled. The current case is quite
280 extreme since most of the analyses have been made more than two years after sampling, but not
281 completely uncommon.

- 282 • Barium sulfate precipitation is a potential mitigation and remediation process to lower the concen-
283 tration of heavy metals and potentially toxic species. Indeed, the concentrations of most trace ele-
284 ments have decreased by several orders of magnitude during the two years period, reaching even-
285 tually concentrations below the detection limit. This can provide an mitigation approach to recycle
286 hydraulic fracturing waters by adding either Ba ions for sulfate rich wastewaters or sulfate in barium
287 rich wastewaters (e.g. Marcellus). The precipitation of barium sulfate (barite) could scavenge a large
288 amount of trace elements and heavy metals from the returned waters decreasing their concentrations
289 below detection limits. Since hydraulic fracturing is using thousands of m³ of freshwater and pro-
290 ducing large amounts of highly saline wastewater, the recycling of such returned waters is a necessity
291 to lower the pressure on water resources and a quick way to reduce the trace elements and heavy met-
292 als concentration could help alleviate this issue. This however means that the potential solids would
293 have to be treated with proper care as they would be incorporating radioactive species (Ra) and heavy
294 metals that were scavenged during precipitation of barite.

295 It is important that values for the heavy metals before barite precipitation in our case were still at
296 low levels. The highest concentrations were between 100 and 200 µg/L. These values, while being higher
297 than the drinking water guidelines (Organisation, 2017), are still orders of magnitude lower than other
298 industrial pollution such as mine tailing (for example As average concentrations of 22.53 mg/L in the
299 polluted groundwater linked to Chéni mine in France Bodénan et al. (2004)). Finally, the combination
300 of barite precipitation with the absence of oxidative breaker and the low initial trace and heavy metals
301 concentrations in formation water leads to high TDS, Na-Cl type, returned waters presenting low to very
302 low concentrations for all minor species and thus low to very low toxicity except for the hypersalinity.

303 **6 Conclusion**

304 The presented study was initially designed to analyze the effect of a new gelling agent for hydraulic frac-
305 turing operations. This new gelling agent does not require an strong oxidative breaker (such as persulfate),
306 which limits the potential water/rock interaction during the hydraulic fracturing and the flowback pe-
307 riod. Water samples were taken during the different periods of the process (coil tubing and flowback) and
308 were analyzed for major and trace elements. Results showed that, as expected, little water/rock interaction
309 occurred except the precipitation of barite.

310 However, due to the high detection limits of the first Argentinian laboratory which analyzed the results,
311 it was decided to duplicate the analyses both at TotalEnergies and at BRGM. Because of custom delays, these
312 additional analyses were performed only 9 months later for some (TotalEnergies) and more than 2 years
313 after sampling (BRGM). These extra results show a systematic decrease in the heavy metal content from the
314 initial analyses. This decrease is interpreted in terms of post-sampling barite precipitation which scavenges
315 heavy metals. This opens an potential mitigation technique for flowback and produced waters to improve
316 their quality and go towards their recycling.

317 **7 Acknowledgment**

318 G. Lebas, M. Burgos Egado, K. Cailleaud, J. Lerat (TotalEnergies, France), M. Lopez, D. Rosenman and D.
319 Gonzales (TotalEnergies Argentina) are warmly thanked for their help and for the concept of the research
320 and the sampling of the flowback waters. Two anonymous reviewers are also thanked for their help in
321 improving the manuscript. The interpretation of the data was done by F. Osselin and co-authors within
322 the framework of the G-baseline project, co-funded by a strategic project grant of the Natural Sciences and
323 Engineering Research Council of Canada (NSERC grant N°463605), the French Research Agency (ANR-14-
324 CE05-0050 grant) and TotalEnergies R& D. This research was undertaken thanks in part to funding from
325 the Canada First Research Excellence Fund.

326 **8 Supplementary Information**

327 Analytical results for the different samples described in this study. When applicable, results from the 3
328 laboratories (INDUSER, TOTAL and BRGM) are mentioned.

Sample	Date DD/MM/YYYY	Time HH:mm	pH -	TDS mg/L	Cl mg/L	Alkalinity mg/L	Na mg/L	Ca mg/L	Mg mg/L
WW3	09/10/2014	-	9.1	1998	444	656	730	4	0.4
WW4	11/10/2015	-	9.1	1264	125	326	415	6.8	0.11
PW	13/10/2015	15:00	6	115795	71000	136	29657	9980	1360
CT1	19/10/2015	10:00	6.3	13978	7410	895	5030	264	30.7
CT2	31/10/2015	07:30	6.7	23824	12500	-	7910	630	66.4
FB1	08/11/2015	11:40	6.5	22999	12482	-	7820	633	62.9
FB2	08/11/2015	16:00	6.9	41996	24740	1180	13550	1350	183
FB3	09/11/2015	09:30	6.4	41858	25000	1480	13210	1130	134
FB4	09/11/2015	16:00	6.4	41790	24760	1340	13590	1060	127
FB5	10/11/2015	09:30	6.3	43982	25150	1460	14910	1290	153
FB6	10/11/2015	16:00	7	42716	25390	1460	13620	1160	143

Table 1: Selected results from the flowback water samples (Induser) - Major elements (<LQ = below quantification limit)

Sample	Date DD/MM/YYYY	Time HH:mm	K mg/L	SO ₄ mg/L	$\delta^2\text{H}$ ‰	$\delta^{18}\text{O}$ ‰
WW3	09/10/2014	-	0.9	253	-88.8	-11.0
WW4	11/10/2015	-	1.3	404	-95.3	-12.3
PW	13/10/2015	15:00	330	<LQ	-33.0	-1.5
CT1	19/10/2015	10:00	41	200	-	-
CT2	31/10/2015	07:30	87	106	-66.5	-5.9
FB1	08/11/2015	11:40	56.2	-	-65.0	-6.0
FB2	08/11/2015	16:00	170	32.8	-53.4	-3.6
FB3	09/11/2015	09:30	139	34.9	-53.7	-4.0
FB4	09/11/2015	16:00	132	35.1	-54.9	-4.1
FB5	10/11/2015	09:30	157	32.5	-	-
FB6	10/11/2015	16:00	147	34.5	-52.8	-3.9

Table 2: Selected results from the flowback water samples (Induser) - Major elements (<LQ = below quantification limit) - Continued

Sample	Date	Time	Ba			Sr			Mn		B			Fe	
			Induser	Total mg/L	BRGM	Induser	Total mg/L	BRGM	Induser mg/L	BRGM	Induser	Total mg/L	BRGM	Induser mg/L	BRGM
WW3	09/10/2014	-	<LQ	-	0.1	<LQ	-	0.174	<LQ	4.42 (µg/L)	0.7	-	0.646	0.64	-
WW4	11/10/2015	-	<LQ	0.18	0.075	<LQ	0.27	0.213	<LQ	9.29 (µg/L)	0.4	0.2	0.189	0.53	-
PW	13/10/2015	15:00	781	734	660	1750	3002	2863.41	13.1	12.489	51.5	43	50.434	173	155
CT1	19/10/2015	10:00	2.9	-	-	63.5	-	-	4.21	-	23.3	-	-	24.2	-
CT2	31/10/2015	07:30	23.9	5.5	4.043	111	145	129.021	5.1	1.668	31.1	30	65.229	97.1	12
FB1	08/11/2015	11:40	26.4	-	-	219	-	-	10.3	-	<LQ	-	-	307	-
FB2	08/11/2015	16:00	131	-	51.804	421	-	306.326	10.6	0.761	79.7	-	51.467	198	-
FB3	09/11/2015	09:30	137	81	55.237	394	335	287.217	8.12	5.313	83	48	52.038	122	125
FB4	09/11/2015	16:00	130	-	59.898	389	-	305.807	7.51	5.490	84.7	-	55.176	121	-
FB5	10/11/2015	09:30	135	-	69.464	382	-	306.514	7.61	5.439	81.2	-	53.577	199	-
FB6	10/11/2015	16:00	145	-	70.472	366	-	316.825	8.08	5.539	-	-	55.589	130	-
Quantification limit			1	0.0005	0.0005	1	0.001	0.001	0.05	0.001	0.2	0.005	0.005	0.2	0.001

Table 3: Selected results from the flowback water samples and evolution between INDUSER and BRGM - Traces elements (<LQ = below quantification limit; - not measured)

Sample	Date	Time	As		Co		Cu		Cr		Ra
			Induser µg/L	BRGM	Induser µg/L	BRGM	Induser µg/L	BRGM	Induser µg/L	BRGM	
WW3	09/10/2014	-	<LQ	1.61	<LQ	<LQ	1.64	<LQ	1.64	-	-
WW4	11/10/2015	-	120	12.28	<LQ	<LQ	<LQ	-	<LQ	<LQ	-
PW	13/10/2015	15:00	210	0.67	<LQ	0.51	<LQ	1.81	<LQ	30.3	137.3
CT1	19/10/2015	10:00	<LQ	-	<LQ	-	<LQ	-	<LQ	-	-
CT2	31/10/2015	07:30	<LQ	0.83	<LQ	1.13	180	<LQ	200	22.9	-
FB1	08/11/2015	11:40	<LQ	-	190	-	240	-	190	-	1.58
FB2	08/11/2015	16:00	<LQ	<LQ	160	1.4	<LQ	1.7	160	25.7	-
FB3	09/11/2015	09:30	100	1.03	<LQ	0.6	<LQ	2.37	<LQ	73.3	-
FB4	09/11/2015	16:00	<LQ	0.96	<LQ	0.51	<LQ	2.49	<LQ	75.5	-
FB5	10/11/2015	09:30	<LQ	4.43	<LQ	<LQ	<LQ	2.59	<LQ	85.8	-
FB6	10/11/2015	16:00	<LQ	1.02	<LQ	<LQ	<LQ	2.57	<LQ	86.0	13.65
Quantification limit			0.10		0.10		0.10		0.10		

Table 4: Selected results from the flowback water samples and evolution between INDUSER and BRGM - Traces elements (<LQ = below quantification limit; - not measured) - Continued

References

- 329 **References**
- 330 Abualfaraj, N., Gurian, P. L., and Olson, M. S. (2014). Characterization of marcellus shale flowback water.
331 *Environmental Engineering Science*, 31:140716083132007.
- 332 Administration, U. E. (2013). Technically recoverable shale oil and gas resources: An assessment of 137
333 shale formations in 41 countries outside the united state.
- 334 Appelo, C. and Postma, D. (2005). *Geochemistry, Groundwater And Pollution, Second Edition*. Taylor &
335 Francis.
- 336 Appelo, C. A. (2015). Principles, caveats and improvements in databases for calculating hydrogeochemical
337 reactions in saline waters from 0 to 200°C and 1 to 1000atm. *Applied Geochemistry*, 55:62–71.
- 338 Bern, C. R., Birdwell, J. E., and Jubb, A. M. (2021). Water–rock interaction and the concentrations of
339 major, trace, and rare earth elements in hydrocarbon-associated produced waters of the united states.
340 *Environmental Science: Processes & Impacts*, 23:1198–1219.
- 341 Birkle, P. (2016). Recovery rates of fracturing fluids and provenance of produced water from hydraulic
342 fracturing of silurian qusaiba hot shale, northern saudi arabia, with implications on fracture network.
343 *AAPG Bulletin*, 100:917–941.
- 344 Birkle, P. and Makechnie, G. K. (2022). Geochemical cycle of hydraulic fracturing fluids: Implications
345 for fracture functionality and frac job efficiency in tight sandstone. *Journal of Petroleum Science and*
346 *Engineering*, 208.
- 347 Blauch, M. E., Myers, R. R., Moore, T. R., and Lipinski, B. A. (2009). Marcellus shale post-frac flowback
348 waters – where is all the salt coming from and what are the implications? *SPE 125740, SPE Regional*
349 *Eastern Meeting*, pages 1–20.
- 350 Board, N. E. (2017). Canada's energy future 2017 supplement: Natural gas production.
- 351 Bodéan, F., Baranger, P., Piantone, P., Lassin, A., Azaroual, M., Gaucher, E., and Braibant, G. (2004).
352 Arsenic behaviour in gold-ore mill tailings, massif central, france: hydrogeochemical study and investi-
353 gation of in situ redox signatures. *Applied Geochemistry*, 19:1785–1800.
- 354 Bondu, R., Kloppmann, W., Naumenko-Dèzes, M. O., Humez, P., and Mayer, B. (2021). Potential impacts

- 355 of shale gas development on inorganic groundwater chemistry: Implications for environmental baseline
356 assessment in shallow aquifers. *Environmental Science and Technology*, 55:9657–9671.
- 357 Brittingham, M. C., Maloney, K. O., Farag, A. M., Harper, D. D., and Bowen, Z. H. (2014). Ecological risks
358 of shale oil and gas development to wildlife, aquatic resources and their habitats. *Environmental Science
359 & Technology*, 48:11034–11047.
- 360 Claret, F., Tournassat, C., Crouzet, C., Gaucher, E. C., Schäfer, T., Braibant, G., and Guyonnet, D. (2011).
361 Metal speciation in landfill leachates with a focus on the influence of organic matter. *Waste Management*,
362 31:2036–2045.
- 363 Crecelius, E., Trefry, J., McKinley, J., Lasorsa, B., and Trocine, R. (2007). Study of barite solubility and the
364 release of trace components to the marine environment.
- 365 Darrah, T. H., Vengosh, A., Jackson, R. B., Warner, N. R., and Poreda, R. J. (2014). Noble gases identify the
366 mechanisms of fugitive gas contamination in drinking-water wells overlying the marcellus and barnett
367 shales. *Proc Natl Acad Sci U S A*, 111:14076–14081.
- 368 (EIA), E. I. A. (2019). Annual energy outlook 2019 with projections to 2050.
- 369 Engelder, T., Cathles, L. M., and Bryndzia, L. T. (2014). The fate of residual treatment water in gas shale.
370 *Journal of Unconventional Oil and Gas Resources*, 7:33–48.
- 371 Essington, M. E. (2005). *Soil and Water chemistry: an integrative approach*. CRC Press.
- 372 Gallegos, T. J. and Varela, B. A. (2015). Trends in hydraulic fracturing distributions and treatment fluids,
373 additives, proppants, and water volumes applied to wells drilled in the united states from 1947 through
374 2010—data analysis and comparison to the literature.
- 375 Gregory, K. B., Vidic, R. D., and Dzombak, D. A. (2011a). Water management challenges associated with
376 the production of shale gas by hydraulic fracturing. *Elements*, 7:181–186.
- 377 Gregory, K. B., Vidic, R. D., and Dzombak, D. A. (2011b). Water management challenges associated with
378 the production of shale gas by hydraulic fracturing. *Elements*, 7:181–186.
- 379 Gupta, J. (1991). Determination of barium, strontium and nine minor and trace elements in impure barite
380 and strontianite by inductively-coupled plasma atomic-emission spectrometry after dissolution in dis-
381 odium ethylenediaminetetraacetate. *Talanta*, 38:1083–1087.

- 382 Hakala, J. A., Vankeuren, A. N. P., Scheuermann, P. P., Lopano, C., and Guthrie, G. D. (2021). Predicting the
383 potential for mineral scale precipitation in unconventional reservoirs due to fluid-rock and fluid mixing
384 geochemical reactions. *Fuel*, 284:118883.
- 385 Haluszczak, L. O., Rose, A. W., and Kump, L. R. (2013). Geochemical evaluation of flowback brine from
386 marcellus gas wells in pennsylvania, usa. *Applied Geochemistry*, 28:55–61.
- 387 Hoke, G. D., Aranibar, J. N., Viale, M., Araneo, D. C., and Llano, C. (2013). Seasonal moisture sources
388 and the isotopic composition of precipitation, rivers, and carbonates across the andes at 32.5-35.5°s.
389 *Geochemistry, Geophysics, Geosystems*, 14:962–978.
- 390 Huang, R., Sun, W., Ding, X., Zhao, Y., and Song, M. (2020). Effect of pressure on the kinetics of peridotite
391 serpentinization. *Physics and Chemistry of Minerals*, 47.
- 392 Humez, P., Osselin, F., Kloppmann, W., and Mayer, B. (2019). A geochemical and multi-isotope model-
393 ing approach to determine sources and fate of methane in shallow groundwater above unconventional
394 hydrocarbon reservoirs. *Journal of Contaminant Hydrology*, 226:103525.
- 395 Johnson, J. D. and Graney, J. R. (2015). Fingerprinting marcellus shale waste products from pb isotope and
396 trace metal perspectives. *Applied Geochemistry*, 60:104–115.
- 397 Kondash, A., Albright, E., and Vengosh, A. (2017). Quantity of flowback and produced waters from uncon-
398 ventional oil and gas exploration. *Science of the Total Environment*, 574:314–321.
- 399 Kondash, A. J., Lauer, N. E., and Vengosh, A. (2018). The intensification of the water footprint of hydraulic
400 fracturing. *Science Advances*, 4.
- 401 Lerat, J. G., Sterpenich, J., Mosser-Ruck, R., Lorgeoux, C., Bihannic, I., Fialips, C. I., Schovsbo, N. H.,
402 Pironon, J., and Éric C. Gaucher (2018). Metals and radionuclides (mar) in the alum shale of denmark:
403 Identification of mar-bearing phases for the better management of hydraulic fracturing waters. *Journal*
404 *of Natural Gas Science and Engineering*, 53:139–152.
- 405 Li, Y., Huang, T., Pang, Z., and Jin, C. (2017). Geochemical processes during hydraulic fracturing: a water-
406 rock interaction experiment and field test study. *Geosciences Journal*, 21:753–763.
- 407 Liu, D., Li, J., Zou, C., Cui, H., Ni, Y., Liu, J., Wu, W., Zhang, L., Coyte, R., Kondash, A., and Vengosh, A.
408 (2020). Recycling flowback water for hydraulic fracturing in sichuan basin, china: Implications for gas
409 production, water footprint, and water quality of regenerated flowback water. *Fuel*, 272:117621.

- 410 Lu, J., Mickler, P. J., Nicot, J.-P., Choi, W., Esch, W. L., and Darvari, R. (2017). Geochemical interactions of
411 shale and brine in autoclave experiments—understanding mineral reactions during hydraulic fracturing
412 of marcellus and eagle ford shales. *AAPG Bulletin*, 101:1567–1597.
- 413 Ni, Y., Zou, C., Cui, H., Li, J., Lauer, N. E., Harkness, J. S., Kondash, A. J., Coyte, R. M., Dwyer, G. S., Liu, D.,
414 Dong, D., Liao, F., and Vengosh, A. (2018). Origin of flowback and produced waters from sichuan basin,
415 china. *Environmental Science and Technology*, 52:14519–14527.
- 416 of Canada, N. E. B. (2018). Neb - canada's energy future 2018: Energy supply and demand projections to
417 2040 - publication information and downloads.
- 418 of Canadian Academies, C. (2014). *Environmental Impacts of Shale Gas Extraction in Canada*.
- 419 Organisation, W. H. (2017). Guidelines for drinking-water quality: fourth edition incorporating the first
420 addendum.
- 421 Osborn, S. G., Vengosh, A., Warner, N. R., and Jackson, R. B. (2011). Methane contamination of drinking
422 water accompanying gas-well drilling and hydraulic fracturing. *Proceedings of the National Academy of
423 Sciences of the United States of America*, 108:8172–6.
- 424 Osselin, F., Nightingale, M., Hearn, G., Kloppmann, W., Gaucher, E., Clarkson, C. R., and Mayer, B. (2018).
425 Quantifying the extent of flowback of hydraulic fracturing fluids using chemical and isotopic tracer
426 approaches. *Applied Geochemistry*, 93:20–29.
- 427 Osselin, F., Saad, S., Nightingale, M., Hearn, G., Desautly, A.-M., Gaucher, E., Clarkson, C., Kloppmann,
428 W., and Mayer, B. (2019). Geochemical and sulfate isotopic evolution of flowback and produced waters
429 reveals water-rock interactions following hydraulic fracturing of a tight hydrocarbon reservoir. *Science
430 of The Total Environment*, 687:1389–1400.
- 431 Parkhurst, D. L. and Appelo, C. (2013). Description of input and examples for phreeqc version 3 — a
432 computer program for speciation, batch-reaction, one-dimensional transport, and inverse geochemical
433 calculations. u.s. geological survey techniques and methods, book 6, chapter a43, 497 p. *U.S. Geological
434 Survey Techniques and Methods, book 6, chapter A43, pages 6–43A*.
- 435 Phan, T. T., Capo, R. C., Stewart, B. W., Graney, J. R., Johnson, J. D., Sharma, S., and Toro, J. (2015). Trace
436 metal distribution and mobility in drill cuttings and produced waters from marcellus shale gas extrac-
437 tion: Uranium, arsenic, barium. *Applied Geochemistry*, 60:89–103.

- 438 Phan, T. T., Hakala, J. A., and Sharma, S. (2020). Application of isotopic and geochemical signals in un-
439 conventional oil and gas reservoir produced waters toward characterizing in situ geochemical fluid-shale
440 reactions. *Science of the Total Environment*, 714:136867.
- 441 Renock, D., Landis, J. D., and Sharma, M. (2016). Reductive weathering of black shale and release of barium
442 during hydraulic fracturing. *Applied Geochemistry*, 65:73–86.
- 443 Rowan, E. L., Engle, M. A., Kraemer, T. F., Schroeder, K. T., Hammack, R. W., and Doughten, M. W. (2015).
444 Geochemical and isotopic evolution of water produced from middle devonian marcellus shale gas wells,
445 appalachian basin, pennsylvania. *AAPG Bulletin*, 99:181–206.
- 446 Scheiber, J., Seibt, A., Birner, J., Cuenot, N., Genter, A., and Moeckes, W. (2014). Barite scale control at the
447 soultz-sous-forêts (france) egs site.
- 448 Thiel, G. P., Tow, E. W., Banchik, L. D., Chung, H. W., and Lienhard, J. H. (2015). Energy consumption in
449 desalinating produced water from shale oil and gas extraction. *Desalination*, 366:94–112.
- 450 Tokunaga, K., Uruga, T., Nitta, K., Terada, Y., Sekizawa, O., Kawagucci, S., and Takahashi, Y. (2016). Ap-
451 plication of arsenic in barite as a redox indicator for suboxic/anoxic redox condition. *Chemical Geology*,
452 447:59–69.
- 453 Vengosh, A., Jackson, R. B., Warner, N., Darrah, T. H., and Kondash, A. (2014). A critical review of the risks
454 to water resources from unconventional shale gas development and hydraulic fracturing in the united
455 states. *Environmental Science & Technology*, 48:8334–8348.
- 456 Warner, N. R., Jackson, R. B., Darrah, T. H., Osborn, S. G., a. Down, Zhao, K., a. White, and a. Vengosh
457 (2012). From the cover: Geochemical evidence for possible natural migration of marcellus formation
458 brine to shallow aquifers in pennsylvania. *Proceedings of the National Academy of Sciences*, 109:11961–
459 11966.
- 460 Xu, M., Binazadeh, M., Zolfaghari, A., and Dehghanpour, H. (2018). Effects of dissolved oxygen on water
461 imbibition in gas shales. *Energy and Fuels*, 32:4695–4704.
- 462 Yang, S., Liu, D., Yang, Z., Wang, C., Chen, X., Li, H., Li, Q., Yang, B., and Li, Y. (2021). Occurrence
463 and mobility of trace elements during oxidant stimulation of shales in yichang, hubei province of china.
464 *Applied Geochemistry*, 127:104913.

Highlights

- New gelling agent presents no water-rock interactions during hydraulic fracturing
- Decrease of trace and heavy metals with time in flowback samples
- Barite precipitation is responsible for this self-remediation

Journal Pre-proof

Credit Author Statement :

F. Osselin: Formal analysis, writing – original draft

E.C. Gaucher : Conceptualization, funding acquisition, formal analysis, writing – review & editing

P. Baldony-Andrey: Conceptualization, funding acquisition

W. Kloppmann: Conceptualization, funding acquisition

B. Mayer: Conceptualization, funding acquisition

Declaration of interests

The authors declare that they have no known competing financial interests or personal relationships that could have appeared to influence the work reported in this paper.

The authors declare the following financial interests/personal relationships which may be considered as potential competing interests:

P. Baldony-Andrey is an employee and E. C. Gaucher is a former employee of TotalEnergies.